Memory for stimulus durations is not bound to spatial information

Wouter Kruijne
Rijksuniversiteit Groningen

Christian N. L. Olivers
Vrije Universiteit Amsterdam

Hedderik van Rijn
Rijksuniversiteit Groningen

Abstract

Different models have been proposed to explain how the human brain derives an accurate sense of time. One specific class of models, intrinsic models, state that temporal information of a stimulus is represented much like other features such as color and location, bound together to form a coherent percept. Here we explored to what extent this holds for temporal information after it has been perceived and is held in working memory for subsequent comparison. We recorded EEG of participants who were asked to time stimuli at lateral positions of the screen followed by comparison stimuli presented in the center. Using well-established markers of working memory maintenance, we investigated whether the usage of temporal information evoked neural signatures that were indicative of the location where the stimuli had been presented, both during maintenance and during comparison . Neural and behavioral measures, including the contralateral delay activity, lateralized alpha suppression and decoding analyses through time, all supported the same conclusion: while the representation of location was strongly involved during the perception of temporal information, once temporal information was committed to memory it no longer showed any relation to spatial information during maintenance or during comparisons. These results support a model where the initial perception of a stimulus involves intrinsic computations, but that this information is subsequently translated to a stimulus-independent format to be used to further guide behavior.

Introduction

Most of our behavior benefits from an accurate sense of time, from holding a fluent conversation with well-timed pauses, to playing music or sports, to navigating traffic. Timing is crucial to determine when to act or when to expect an upcoming event. Therefore, understanding the mechanisms, processes and representations of time and durations in the

brain are essential aspects of understanding human cognition and behavior as a whole. To this end, a wide array of competing models and theories have been proposed: One of the most recent review articles lists eighteen different models (Addyman, French, & Thomas, 2016; see also Hass & Durstewitz, 2014), each relying on different assumptions and computations.

Models of timing are typically evaluated and constrained on the basis of errors and biases in time perception displayed by both humans and other animals. For example, the 'scalar property' describes that variability in perceived duration is proportional to the objective duration (Gibbon, 1977; Hass & Herrmann, 2012; Kacelnik, Brunner, & Gibbon, 1990; Malapani & Fairhurst, 2002). As this is so commonly found in both human and nonhuman timers this has been described as a hallmark of interval timing models (Buhusi & Meck, 2005; Okamoto & Fukai, 2001). Other factors that are typically considered include how time perception is affected by the physical properties of the timed stimulus (Eagleman, 2008; Schlichting, de Jong, & van Rijn, 2018; Walsh, 2003), the contextual or emotional salience of the stimulus (Allman, Teki, Griffiths, & Meck, 2014; Droit-Volet & Meck, 2007; Ernst et al., 2017; Halbertsma & Rijn, 2016; Matthews, 2011), the influence of past timing experiences (Jazayeri & Shadlen, 2010; Lejeune & Wearden, 2009; Maaß, Schlichting, & van Rijn, 2019; Roach, McGraw, Whitaker, & Heron, 2017; Schlichting, Damsma, et al., 2018; Taatgen & van Rijn, 2011), and how temporal percepts are affected by neuropharmacological substances (Coull, Cheng, & Meck, 2011; Meck, 1996; Soares, Atallah, & Paton, 2016) or aging processes (Lustig & Meck, 2001; Maaß, Riemer, Wolbers, & van Rijn, 2019; Turgeon, Lustig, & Meck, 2016).

While such studies have yielded important constraints on the dynamic computations that underlie a temporal percept, much fewer studies have directly investigated the actual representation of this percept. Consider, for example, the simple task of sequentially perceiving two intervals of different durations, followed by the question: "which interval lasted longer?" Such a task will not only involve the perception of time, but also requires one to commit some representation of the first duration to memory in a manner that it is then usable for comparison with the second interval. The present study aims to investigate the nature of this representation.

With respect to this representation, the wealth of models and theories on timing can be coarsely divided into two classes. In *dedicated* clock models (e.g. Gibbon, 1977; Gu, van Rijn, & Meck, 2015; Matell & Meck, 2004; van Rijn, Gu, & Meck, 2014), the representation of time is functionally decoupled from the imperative stimulus. These models assume that sensory events are processed and subsequently fed into a largely independent timing system. Sensory information serves to signal the onset or offset of an interval, and might in some models, trigger or modulate internal dynamics that give rise to the temporal percept. However, the end result of timing is represented by a dedicated circuit and is in itself not linked to the presented stimulus or any of its features. For example, the Striatal Beat Frequency model assumes that the representation of time derives from a concert of oscillatory activity at slightly different frequencies, which are reset by the perceived onset of an interval. Whenever time is to be read out and committed to memory, it is represented by the state of the peaks and troughs in each frequency band. This representation is completely independent from the stimulus that initially triggered the oscillations.

By contrast, *intrinsic* clock models (e.g. Finnerty, Shadlen, Jazayeri, Nobre, & Buono-

mano, 2015; French, Addyman, Mareschal, & Thomas, 2014; Mauk & Buonomano, 2004; Paton & Buonomano, 2018) assume that the representation of time is a product of the stimulus percept itself. In these models, perceiving the stimulus triggers dynamics that are intrinsically part of a stimulus representation, just like features such as location and shape, but that can be used to infer time. In some models, such as the Temporal Context Model (Shankar & Howard, 2010; and its successors Shankar & Howard, 2011, 2013) and the Gaussian Activation Model of Interval Timing (French et al., 2014), the perceived time of an interval is directly derived from its representation in memory. These models typically assume that the stimulus representation is not static but gradually changes as a function of time, which endows these representations with the capabilities of an intrinsic clock.

While dedicated and intrinsic clock models differ in their assumptions regarding the representations and dynamics involved in the perception of duration, models of both classes assume that in a comparison task, the duration percept must somehow be committed to memory. As such, the nature of working memory for time poses important implementation constraints for all models of timing. Nevertheless, models typically make no claims about how temporal information is represented in working memory. Therefore, here we attempt to map this representation by means of electroencephalography (EEG). In particular, we will measure lateralized signals that are ubiquitously studied in visual working memory research and which suggest that space might be a crucial dimension to bind features of representations in memory. Here, we investigate whether these spatial signatures can also be observed when durations are to be maintained.

The first of these signatures is the Contralateral Delay Activity (CDA), a component in the event-related potential (ERP) that was originally identified in change detection experiments (Eimer & Kiss, 2010; Ikkai, McCollough, & Vogel, 2010; Luria, Balaban, Awh, & Vogel, 2016; Vogel & Machizawa, 2004). When participants are required to remember items presented on one side of the screen, then a sustained occipital contralateral negativity is observed. The amplitude of this component can be related to the memory load on the trial, and to the memory capacity of the participant. Interestingly, a CDA is also found in studies where the location of the remembered stimulus is irrelevant for the upcoming task, for example when the stimulus is to be used in visual search (Carlisle, Arita, Pardo, & Woodman, 2011; Woodman, Carlisle, & Reinhart, 2013) or merely has to be recognized in the center of the screen (Gunseli, Olivers, & Meeter, 2014). Together with the CDA-component found in the ERP, working memory for laterally presented items is often found to yield a contralateral suppression of frequency power in the alpha band (Klimesch, 2012; Mazaheri, 2010; Van Driel, Gunseli, Meeter, & Olivers, 2017). Such lateralized alpha suppression has been linked to both maintenance of items in working memory, as well as covertly attending a location in space (Diepen, Miller, Mazaheri, & Geng, 2016; Foster, Sutterer, Serences, Vogel, & Awh, 2017; Sauseng et al., 2005; van Moorselaar et al., 2018).

Lateralized neural signatures have not only been found for memory *maintenance* but similarly for when visual information is *retrieved* from memory. The N2pc is an occipital contralateral negative inflection of the ERP typically found 200–350ms after a stimulus, that is assumed to reflect attentional orienting (Eimer, 1993; Eimer & Grubert, 2014; Luck, Fan, & Hillyard, 1993; Luck & Hillyard, 1994; Tan & Wyble, 2015). While the N2pc is classically studied in the context of visual search, various studies have reported that retrieving lateralized stimuli from working memory similarly evokes an N2pc (Dell'Acqua, Sessa, Toffanin,

Luria, & Jolicœur, 2010; Kuo, Rao, Lepsien, & Nobre, 2009; Leszczyński, Myers, Akyürek, & Schubö, 2011). Much like these effects on the ERP, orienting to endogenous representations in working memory has been found to produce lateralized suppression of alpha-band power. In these cases, alpha power is found to be suppressed, contralateral to the side that an item that was presented that either has just become relevant or is expected to become relevant. In most studies such orienting is explicitly triggered by means of retro-cues (Poch, Campo, & Barnes, 2014; van Ede, 2018; Wolff, Jochim, Akyürek, & Stokes, 2017), but it is also observed in experiments where a sequence of subtasks sequentially requires the activation of a different item from memory (de Vries, Van Driel, & Olivers, 2017, 2019). Particularly relevant to the present research, orienting responses in the alpha band have also been found in a task where no explicit cues for retrieval are given, but where instead the duration of the memory delay itself informed participants which of two memory items is more likely to be tested (van Ede, Niklaus, & Nobre, 2017).

These findings constitute lateralized signatures of maintenance and retrieval of working memory items. Crucially, in many if not most of these studies, lateralized EEG-responses were found despite the fact that spatial information was itself irrelevant for the task: often only non-spatial features of these items, such as color or orientation needed to be maintained. These findings suggest that the memory representation of visual features inherently includes spatial information, which is subsequently detected in the EEG. The visual cortex inherently has a spatiotopic organization, and space is a primary binding dimension in many computational models of working memory storage (Oberauer & Lin, 2017; Schneegans & Bays, 2017; Swan & Wyble, 2014). Therefore, we reason that if the working memory representation of time is similarly bound to sensory information, these spatial neural signatures would be the most likely markers to detect such binding.

Specifically, participants were sequentially presented with two intervals (Interval 1 and Interval 2), separated by a memory delay. Participants subsequently had to determine which of the intervals was longer. Each interval was presented by means of visual markers: stimuli that were briefly presented to indicate the start- and the end-signal for timing. Critically, for Interval 1 these markers were lateralized, that is, presented on either the left or right side of the display, whereas the markers for Interval 2 were both presented in the center. If temporal information uses a representation that is bound to spatial information, then we should be able to find lateralized EEG-signals indicative of maintenance, retrieval or anticipation during the centrally presented second interval. In that case, their dynamics and their timing could be informative of how such a comparison task is solved: for example, temporal information might be retrieved either only at the start or end of Interval 2, or might be held active throughout comparison. Furthermore, signals of retrieval might reflect *anticipation* of the start- or end of Interval 2 (cf. van Ede et al., 2017), or they might be evoked *in response* to the stimuli marking its duration (cf. Kuo et al., 2009).

To further disentangle the precise role of memory representations in such a comparison task, we additionally manipulated the manner in which Interval 1 was presented. In blocks with 'Same' trials , the start- and end-marker were presented in the same location, whereas in 'Opposite' blocks, they were on opposite sides. If we observe lateralized neural responses in both of these block types, then the direction of such lateralization could help us identify whether this reflects retrieval of the start-moment, the end-moment or both. Should we only observe lateralization in the EEG in 'Same' blocks, then this might point to a representation

where the interval duration as a whole is bound to one location in space, and retrieved during comparison. Additionally, we sought to relate neural responses to behavior, and contrast correct- and incorrect trials. If the representations underlying lateralized neural signatures are a functional aspect of memory for time, then we expect these neural responses to be weaker or absent on incorrect trials.

Method

Participants. We collected data from 24 healthy participants with normal or corrected-to-normal vision, who were recruited through the participant pool of the Faculty of Behavioral and Movements Sciences of the Vrije Universiteit Amsterdam. All participated for course credits or monetary compensation (€10/hour). Data of four participants were discarded after EEG data preprocessing (described below), two of which due to the number of noisy channels (8 and 10 electrodes) and two due to the high percentage of discarded data segments (38% and 52%) due to contamination from muscle artefacts or horizontal eye movements. No participants were excluded based on behavior. We inspected behavioral performance, we fit an individual logistic regression model to the proportion of 'longer' responses as a function of Δt = (Interval 2 - Interval 1), and all slope coefficients were less than 2 SD away from the group mean. The final sample contained 20 participants (ages 19–26, Mean age 21.9, 10 female). For all participants, informed consent was obtained before participation, and all procedures during the experiment were in accordance with the Helsinki declaration. The protocol was approved by the ethical review board of the Faculty of Behavioral and Movement sciences of the Vrije Universiteit Amsterdam.

Procedure and stimulus presentation. Participants were seated in a darkened, sound-attenuated room at 75cm viewing distance from a 22 inch screen (Samsung Syncmaster 2233, 1680 × 1050 resolution, 120 Hz refresh rate). The experiment was programmed and presented using OpenSesame (Mathôt, Schreij, & Theeuwes, 2012), using the PsychoPy back-end (Peirce, 2007). The stimulus sequence of a trial is schematically depicted in Figure 1 (with gray and black colors inverted for visibility). Trials started with a gray fixation cross (0.2°), on on a black background for 1000ms, followed by the onset of three, horizontally aligned gray placeholder circles (radius 1.97°, one in the center and two at 9.83° eccentricity) around a central gray fixation dot (0.2°). The placeholders and fixation dot stayed on screen until the end of the trial.

The presentation of Interval 1, the 'standard interval', started 500ms after placeholder onset, and was indicated by an onset- and offset marker flashing (125ms) in either the left or right placeholder. Both markers were red diamonds (3.94° width and height). Their SOA defined the standard interval, and was a value randomly sampled from a uniform distribution $\mathcal{U}(1250 - 2250ms)$. After the offset marker was presented, a 1250ms memory delay followed. Interval 2, the 'comparison interval', was similarly indicated by means of an onset- and offset marker, each a green square (sides 2.79°; 125ms) presented in the central placeholder circle. Interval 2 was either shorter or longer than Interval 1, by either 10% or 20%. The offset marker of Interval 2 was followed by a 1250ms response delay. The shape and color of the interval markers were chosen so that Interval 1 and Interval 2 would not share any non-temporal features that might automatically trigger the retrieval of spatial information. The minimum duration between stimuli, 1250ms, was chosen to

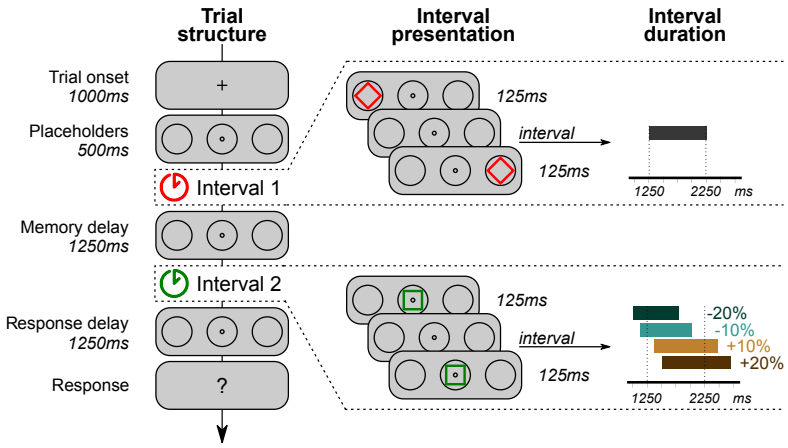

Figure 1. Schematic representation of the design. The general trial structure is depicted on the left, from top to bottom. The middle column depicts the presentation of Interval 1 and Interval 2 by means of their onset- and offset markers. This example illustrates an 'Opposite' trial. For Interval 2, both markers were in the center. The rightmost figures depict the interval distributions: Interval 1 was sampled from a uniform distribution ranging from 1250 to 2250ms; Interval 2 was derived from Interval 1. Note that in the experiment, fixation- and placeholder stimuli were gray on a black background (here inverted for legibility)

be long enough for the relatively sluggish lateralized alpha response to emerge and resolve completely (de Vries, Van Driel, Karacaoglu, & Olivers, 2018; Van Driel et al., 2017).

Participants were instructed to maintain fixation on the center of the screen throughout the trial and not to move their eyes towards the peripheral stimuli. They were asked to compare the duration of the stimuli and determine whether the second interval was shorter or longer than the first. Once the response screen appeared, they could indicate their answer by pressing 'Z' or 'M' on a standard QWERTY keyboard with their left or right index finger. On each trial, the mapping of these keys varied unpredictably and was unknown to the participant until the response screen appeared. This was done to prevent any (lateralized) motor preparation signals contaminating the EEG. On the response screen, the options (Z and M) were presented centrally above or below fixation accompanied by the words "shorter" (above fixation) or "longer" (below). Participants were instructed to prioritize accuracy over response speed.

Participants completed eight blocks of 40 trials each. Before each block, participants were informed whether Interval 1 would be presented via markers on the 'Same' or 'Opposite' sides. Note that regardless of block type, participants could not predict the location of the onset marker, but after its presentation, the location of the offset marker was fully predictable. All combinations of the percentage change and the onset location of Interval 1 were presented five times per block in a random order. The order of Block types (Same/Opposite) alternated and their order was counterbalanced across participants. Before starting the experiment, participants completed practice blocks with Same and Opposite marker presentations, ten trials each. Practice trials were not considered in any of the analyses.

EEG acquisition and data cleaning. EEG data were recorded at 512Hz from 64 channels (BioSemi, Amsterdam, The Netherlands; ActiveTwo system, 10–20 placement; biosemi.com), with two additional electrodes placed at the earlobes, two placed 2cm above and below the right eye, and two electrodes placed 1cm lateral to the external canthi. All offline analyses and data cleaning steps were performed using MNE-python (Gramfort et al., 2013; Gramfort et al., 2014) and R (R Core Team, 2018). EEG data were re-referenced to the average of the data from the earlobes, and V/HEOG traces were created by subtracting data from the opposing channels around the eyes.

For data cleaning, three filtered versions of the raw dataset were created by means of zero-phase FIR filters: band-passed at at 110–140Hz to highlight muscle artefacts; high-passed at 1Hz, removing medium-slow drifts to be used for independent component analysis (ICA); and one high-pass filtered at 0.1Hz to be used for the main analyses. Most algorithms that were used for data cleaning assume epochs of equal length reflecting "trials" as their input. Unless otherwise specified, we used "preprocessing epochs" for these algorithms based on the shortest possible interval durations (1250ms and 1000ms for Interval 1 and 2 respectively) and the fixed 1250ms memory delay between them. These epoch thus spanned -2500ms – 2250ms around the onset of Interval 2. Thresholds and filters that were derived based on these preprocessing epochs were then applied to the entire dataset.

Following the PREP-pipeline (Bigdely-Shamlo, Mullen, Kothe, Su, & Robbins, 2015) we first identified excessively noisy channels by means of the RANSAC algorithm, as implemented by the 'autoreject' package (Jas, Engemann, Bekhti, Raimondo, & Gramfort, 2017). This procedure generates permutations of the epoched data, and predicts full channel activity by interpolating data from a subset (25%) of the channels. If the correlation between the observed and interpolated data is less than a threshold value ($r < 0.75$) in more than 40% of the epochs, the channel is classified as 'bad'. In our dataset, the algorithm identified 6 (n=1), 4 (n=1), 2 (n=2), and 1 (n=3) faulty channels per participant, which were found to be in agreement with visual identification. Faulty channels were primarily located on more peripheral electrode sites, and did not overlap with the preselected electrodes of interest at parieto-occipital sites. We excluded these channels from all other preprocessing steps.

To identify data contaminated by muscle artefacts, we used a procedure adopted from the PREP-pipeline (Bigdely-Shamlo et al., 2015) also offered by FieldTrip (Oostenveld, Fries, Maris, & Schoffelen, 2011). Using the 110–140Hz band-passed dataset, we computed its Hilbert envelope and convolved the result with a 200ms boxcar averaging window. This yielded a per-channel time course estimate of high-frequency power in the original signal. Across all data in the preprocessing epochs, we computed a per-channel median and median absolute deviation, and used these to compute a robust Z-score for all data inside and outside these epochs. Data at time points where the Z-score averaged across channels exceeded 5.0 were marked as contaminated and were not considered in future analyses.

ICA was used to identify and remove artefacts in the data caused by eye blinks. We first subsampled the high-pass filtered (at 1Hz) dataset at 102.4Hz ($=\frac{512}{5}$), and computed independent components (using extended-infomax ICA, the default in EEGLAB; Delorme & Makeig, 2004). From the resulting spatial components, we visually identified those corresponding to blinks. To confirm the validity of this approach, we defined 'blink epochs', as 1000ms windows around local maxima in the 1–10Hz band-passed VEOG signal. The time course of the selected ICA components, and only these components, had a high correlation

with the VEOG signal in these epochs ($r^2 > .5$).

To identify horizontal eye movements, we used a procedure inspired by methods from ERPLAB (Lopez-Calderon & Luck, 2014): Data from the HEOG signal were high-pass filtered at 1Hz, and convolved with a stepwise kernel, defined by 150ms each of -1 and +1 values, with a 25ms linear ramp between them. In the resulting signal, local maxima that exceeded the 99th percentile were marked as potential horizontal saccades. Data from the start of such a mark to the end of the current trial were excluded from further analyses.

The autoreject algorithm (Jas et al., 2017) was used on the preprocessing epochs in order to identify trials with unreasonably high amplitude fluctuations. This algorithm improves on typical epoch rejection methods that use a fixed threshold, and instead estimates optimal channel-specific thresholds by means of cross-validation methods inspired by RANSAC. In epochs where a channel's peak-to-peak value exceeds its threshold, autoreject will initially attempt to interpolate that channel's data from neighboring channels. Only if the number of to-be-corrected channels in an epoch is above an additionally fit integer k, the entire epoch is rejected. We fit autoreject on the preprocessing epochs to find individual thresholds, and report these in the Supplementary Information (https://osf.io/7gpka/)

Using the results of these preprocessing algorithms, we created 'cleaned' data epochs around moments of interest. In each trial, four epochs were defined with data surrounding the presentation of each marker: the onset/offset of Interval 1 and the onset/offset of Interval 2 (Table 1; top row of Figures 3A-D). Time windows were chosen to be maximally long without overlapping with other markers (Table 1). As a consequence, onset- and offset-locked intervals contain partially overlapping data, with the amount of overlap dependent on the interval duration. For each of these time windows, 'cleaned' epochs were created: first, the raw dataset (high-pass filtered at 0.1Hz) was loaded after which the ICA components related to blinks were removed. Data epochs were extracted, where epochs were dropped if they contained muscle artefacts or if they contained data following a horizontal eye movement on the same trial. The autoreject algorithm was then applied to interpolate data with extreme peak-to-peak amplitudes or drop rejected epochs. Finally, data from faulty channels as identified by RANSAC were interpolated on the basis of the neighboring channels. The resulting number of clean epochs per participant used in all analyses is given in online Supplementary Information.

Epoch / Event	$t_{\min}$	$t_{\max}$	Includes		
Onset Interval 1	-1250	1250	Placeholder onset,	Onset marker,	Start Interval 1
Offset Interval 1	-1250	1250	End of Interval 1,	Offset marker,	Memory delay
Onset Interval 2	-1250	1000	Memory delay,	Onset marker,	Start Interval 2
Offset Interval 2	-1000	1250	End of Interval 2,	Offset marker,	Response delay

Table 1
Epoch definition

Event related potentials. To construct ERPs, all epochs were baseline corrected by subtracting the average data of each channel in the 100ms leading up to the onset of the placeholders. [1]. We then computed two average signals for the electrode clusters [P7, P5,

[1] Another approach would be to subtract pre-stimulus baseline activity for each marker separately. That approach is better suited to isolate effects in the transient evoked responses post-stimulus, but is likely

PO7, PO3, P3, P1] and [P8, P6, PO8, PO4, P4, P2] (Figure 3, insets). These electrodes were selected on the basis of earlier work (de Vries et al., 2017, 2019; Van Driel et al., 2017), and corresponded to the visually identified locus of peak lateralized responses. We subtracted the two signals (contralateral-ipsilateral) on each trial to yield an occipito-parietal difference signal. For epochs around the onset- and offset of Interval 2, with centrally presented markers, 'contralateral' and 'ipsilateral' were defined based on the onset- and offset location of Interval 1. Subsequently, ERPs were computed per participant per condition as averages across trials.

Time-frequency analyses. For the same four epochs we computed time-frequency spectra, for the frequencies $F = 2$ to $40Hz$, in 25 geometrically spaced steps. To prevent edge-artifacts, the spectra were computed over epochs that were 1.0s wider than the data of interest. Before computing the spectrum, the overall evoked response was subtracted from the individual data epochs. We used multitaper filtering , using 500ms windows tapered with three Slepian windows and subsequently zero-meaned. Data and filters were convolved by multiplication in frequency space after fast-fourier transformation. Time-frequency data were cropped to align with the ERP-epochs and sub-sampled to 102.4Hz ($=\frac{512}{5}$). Power was baselined and converted to decibel (dB) with respect to the per-trial average power 300-100ms before the onset of the placeholders.

As for the ERPs, spatially averaged frequency power was computed for contralateral and ipsilateral occipito-parietal channels, and their subtraction yielded a measure for power lateralization. In addition, we computed the time course of lateralized alpha power, by averaging data across frequencies between 7 and 13 Hz.

Classification analyses. Using a classification analysis, we investigated whether information regarding marker locations was maintained or retrieved in a manner that was not reflected in lateralized parieto-occipital ERPs. To this end, we trained logistic classifiers to predict the location of the onset- or offset marker from the 64-channel EEG data. As input to these classifiers, we used the epoched data, low-pass filtered at 35Hz and subsampled to 64Hz. Classifiers were trained on 125ms sliding window segments of data (8 time points $\times$ 64 channels) which were Z-scored and used as input features. This setup was constructed to produce high classification accuracy for decoding the onset marker of Interval 1, and was subsequently applied to the other epochs. Classifier performance was evaluated on the basis of 10-fold stratified cross-validation, and scored using the area under the curve (AUC) of the receiver-operator curves. A perfect classification would yield a score of 1.0, and 0.5 reflects chance-level decoding.

Statistics. Participants' behavior on the task was characterized by means of General Linear Mixed-Effects regression (Baayen, Davidson, & Bates, 2008). Models were constructed to predict which of the two intervals was perceived as longer by means of logistic regression with predictors including: the length of Interval 1, the length of Interval 2, their absolute difference (in seconds), their proportional difference (percentage change), and block type (Same/Opposite presentation). All models with different combinations of these predictors, with and without interactions between main effects, were compared by means of their BIC scores. We report the resulting best model, and report statistical evidence for

to obscure potential slow-wave lateralization differences that might still be present right before stimulus presentation (like the CDA). We have ran analyses where epochs were re-baselined as such, but these did not lead to different conclusions

or against effects (likelihood ratio test χ^2 statistic, corresponding p-value, and ΔBIC) by comparing nested models that either included or excluded the effect under consideration.

The ERP, time-frequency- and classification analyses on EEG data were initially all done per-subject. The outcomes of these steps were subsequently subjected to group-level statistical testing using cluster-based permutation tests (Maris & Oostenveld, 2007). Clusters were defined as regions adjacent in time, frequency, and space where univariate statistical testing yielded a p-value lower than 0.05. Low-variance t-values were corrected for using 'hat' variance adjustment (Ridgway, Litvak, Flandin, Friston, & Penny, 2012) with a correction factor $\delta = 0.001$. Cluster size was defined as the sum of all t-values in a cluster, and the maximum cluster sizes found in each out of 5000 permutations were saved to construct a nonparametric null distribution. An observed cluster was considered statistically significant with respect to this distribution at $\alpha = 0.05$.

Results

Behavior

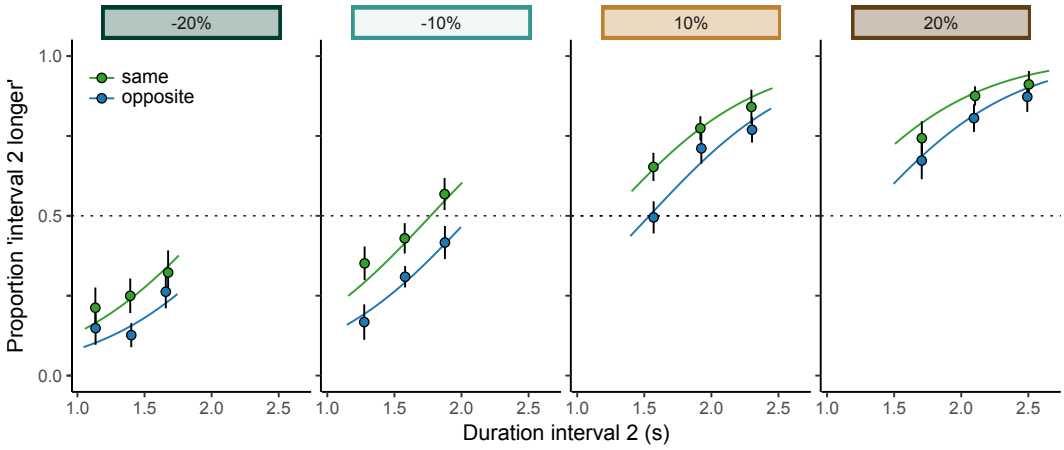

Figure 2. Proportion of trials where participants perceived Interval 2, the comparison interval, as longer. Curves reflect responses predicted by the preferred statistical model with three predictors: the percentage change, Interval 2 duration, and block type (Same/Opposite). For comparison, the data points reflect the proportion of 'longer' responses in three 'Interval 2 duration' bins defined separately per 'percentage change' condition. Error bars reflect 95% within-subject confidence intervals (Cousineau, 2005; Morey, 2008).

The best model predicted 'longer' responses as a function of three additive main effects (Figure 2). First, responses depended on the percentage change, included in the model as a linear predictor ($\chi^2(1) = 23.8, p < 0.001, \Delta BIC = 15.0$). This captures participants' ability to accurately perform the task: that is, a higher proportion of 'longer' responses was generated for trials that were indeed longer, with more certainty for the 20% change than the 10% change conditions.

Second, participants were more likely to respond 'longer' on trials where the second interval was physically long, regardless of how it related to Interval 1 ($\chi^2(1) = 298.8, p < 0.001, \Delta BIC = 296.0$). This suggests that participants at least in part made a decision based on the absolute duration of Interval 2, regardless of Interval 1. Although this could reflect participants' poor memory for Interval 1 on some trials, note that it could also reflect a strategic weighting of evidence: in the present task, the absolute duration of Interval 2 is a good heuristic to determine whether the interval is relatively longer too (see Figure 1, 'Interval duration').

Third, we found that participants' judgments were modulated by the manner of presentation of Interval 1. In blocks where the markers of Interval 1 were on the same side of the screen, participants were more likely to respond that Interval 2 was longer compared to blocks where the markers were on opposite sides. This was an unexpected but highly consistent finding ($\chi^2(1) = 91.2, p < 0.001, \Delta BIC = 82.5$). Conversely, this implies that when Interval 1 was presented with opposite markers, its duration was perceived as longer. In our EEG-analyses, we found that this bias was associated with differing neural responses to the offset markers of Interval 1 between different presentation conditions. Here, we will not explore this particular finding in-depth, as it does not immediately relate to our research question. Instead, our analyses will focus on the neural markers for memory maintenance and retrieval.

ERP analyses

Figure 3 depicts the ERP waveforms during the epochs surrounding the onset- and offset markers of Interval 1 (A,B) and Interval 2 (C,D). The top row of each sub-figure schematically illustrates the sequence of events during the epochs for an illustrative 'Opposite' trial. Note that for the centrally presented Interval 2, 'ipsilateral' and 'contralateral' electrodes are defined with respect to the corresponding marker location during Interval 1.

Onset Interval 1. Figure 3A depicts the ERP in response to the onset of Interval 1. The top plot depicts the ERP of contralateral and ipsilateral electrodes, and their difference. At $t = -500$ms, the onset of the placeholders yields a large visual response in both hemispheres. The lateralized onset marker at $t = 0$ms yields an early lateralized response, offset by an early (90-145ms) significant positivity. Interestingly, this was later followed by another significant contralateral positive component (305–482ms). While we had expected to find a negative component here (the N2pc), there are reported conditions where this component reverses, which we will come back to in the Discussion. After this initial positive inflection, however, this gradually begins to transform into a negative component starting at approximately 400ms, yielding a sustained negativity marked by two significant clusters (594–1076ms)[2]. This sustained negativity matches the typical profile of the CDA.

When the data from 'Same' and 'Opposite' blocks were separately assessed, these conditions yielded virtually equivalent ERPs. The same held when contrasting ERPs on correct versus incorrect trials (bottom plot).

Offset Interval 1. The grand-average ERP surrounding the offset of Interval 1 (Figure 3B, top plot) had a shape that was very similar to that of the onset, although

[2]in this and all subsequent descriptions, we will treat adjacent clusters as one 'effect' if they are less than 50ms apart and denote effects in the same direction.

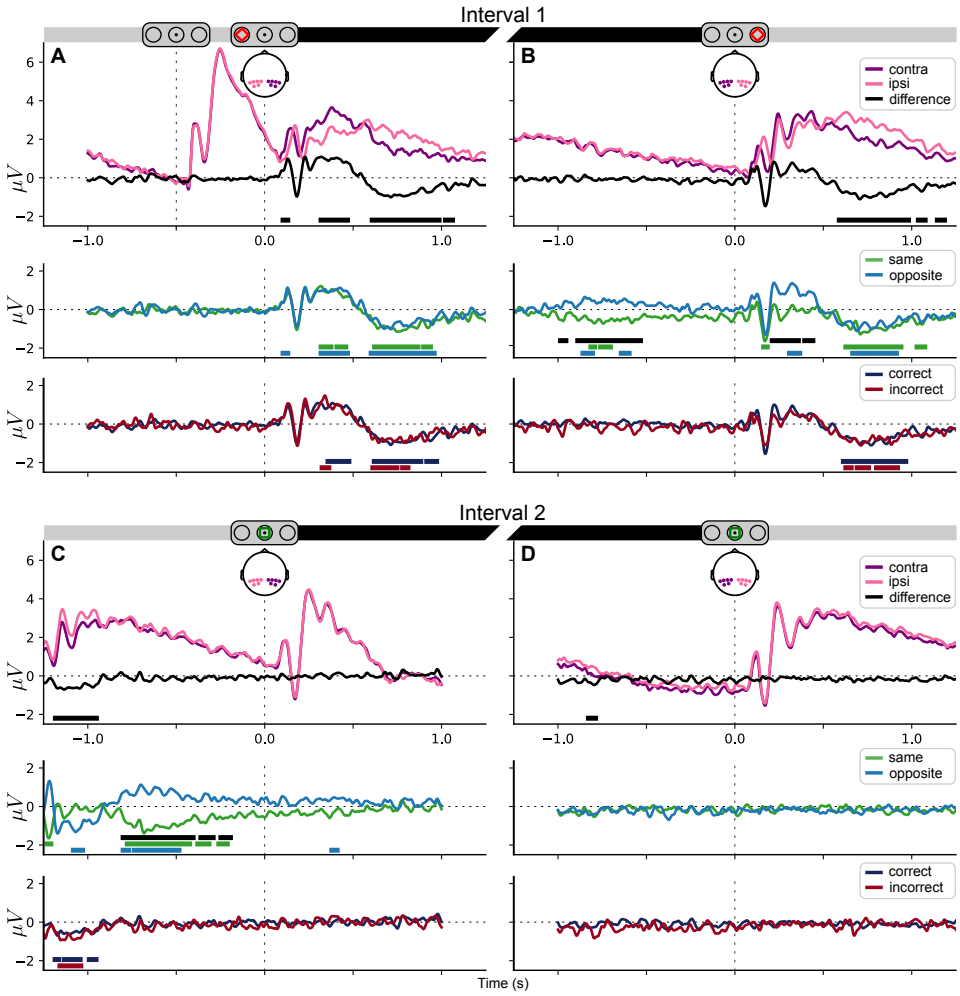

Figure 3. Occipital, lateralized ERPs during epochs around **A** the onset of Interval 1; **B** the offset of Interval 1; **C** the onset of Interval 2; and **D** the offset of Interval 2. Subplots from top to bottom depict overall ERPs, in 'Same' or 'Opposite' trials, and in correct versus incorrect trials. Data were low-pass filtered at 35Hz for visualization only. Colored horizontal line segments indicate clusters significantly different from 0; black segments indicate clusters with condition differences.

none of the early positive and negative inflections were found to be significant here. Again, a sustained late contralateral negativity was found, marked by three significant clusters between 576 and 1199ms.

Here, there were two notable differences between Same and Opposite presentation conditions. First, we found tentative evidence that the CDA evoked at the onset persisted throughout Interval 1. Qualitatively, the ERPs in Same and Opposite conditions emerged as mirror images, consistent with lateralized memory representations of the onset marker. This is supported by a significant cluster indicating a condition difference that persisted from -1000 to -520ms, accompanied by significant clusters in either condition indicating

opposite lateralization within that same time window. No significant differences were found in the final 500ms of the interval, although numerically, lateralization persisted. Second, in response to the offset marker, an early lateralized positivity was found for 'Opposite' but not for 'Same' presentations, with a significant difference between them from 197 to 455ms. In part, this difference might be accounted for by the CDA difference described above, which numerically persisted up to the offset marker. However, after re-baselining the epochs with respect to data just before the offset marker, we still found a significant difference. This transient difference therefore probably reflects a stronger visual evoked response to the offset marker in Opposite blocks than in Same blocks. This makes this neural response a prime candidate neural correlate to drive the behavioral bias that intervals with opposite markers are perceived to last longer. Note that despite this early modulation, after approximately 500ms there was no longer any apparent difference between these conditions: both showed a sustained CDA of similar amplitude with respect to the location of the offset stimulus which persisted persistent throughout the memory delay.

Again, no differences were found between the ERPs on correct trials compared to incorrect trials.

Onset Interval 2. Figure 3C depicts ERP waveforms throughout the delay interval followed by the onset of Interval 2 at $t = 0$ms. Note that Interval 2 markers were not lateralized. At the start of this epoch, the grand average waveforms still reflect the responses following the offset of Interval 1, and therefore show a significant lateralization between -1197 and -938ms. However, for the majority of the delay, the grand average waveform does not reveal any lateralization. The onset of Interval 1 yielded a strong visual response, but this response was equally large for (originally) contralateral and ipsilateral sites, with no evidence for lateralization, neither in the early evoked response nor in the form of later, slow-wave modulations.

This interpretation is supported by the contrast between block types (Same/Opposite presentations). Note that during the delay interval, the ERPs are virtually identical to those in Figure 3B, but with the polarity reversed for the 'Opposite' condition. This results in three significant clusters marking the difference between them, from -814 to -180ms, paired with significant positive and negative lateralization for both conditions in that same time range. Qualitatively, this remnant of the Interval 1 CDA appears to persist up to 500ms into Interval 2, which resulted in a brief significant cluster for the ERP of 'Opposite' blocks (365–424 ms).

The ERPs contrasting correct and incorrect trials again revealed no differences between them.

Offset Interval 2. The average ERPs surrounding the offset of Interval 2 (Figure 3D) similarly showed no evidence for memory-related lateralized responses during the interval. One, short-lived significant cluster was found between -842 and -773 ms, which again most likely reflects a CDA remnant of Interval 1 as depicted in Figure 3C. When separately considering 'Same' and 'Opposite' blocks, no qualitative differences were observed, and no significant clusters were found to suggest lateralization in either condition, nor a difference between conditions. A similar pattern was found for the ERPs on correct versus incorrect trials, which once again revealed no significant differences between them.

To conclude, our ERP results indicate that actively timing an interval marked by laterally presented stimuli is paired with CDA components resembling maintenance of these

markers, suggesting that these stimuli are stored and maintained in memory. However, the ERPs yield no evidence that this memory representation is then subsequently used at retrieval, that is, during the centrally presented comparison interval.

Time-frequency decomposition

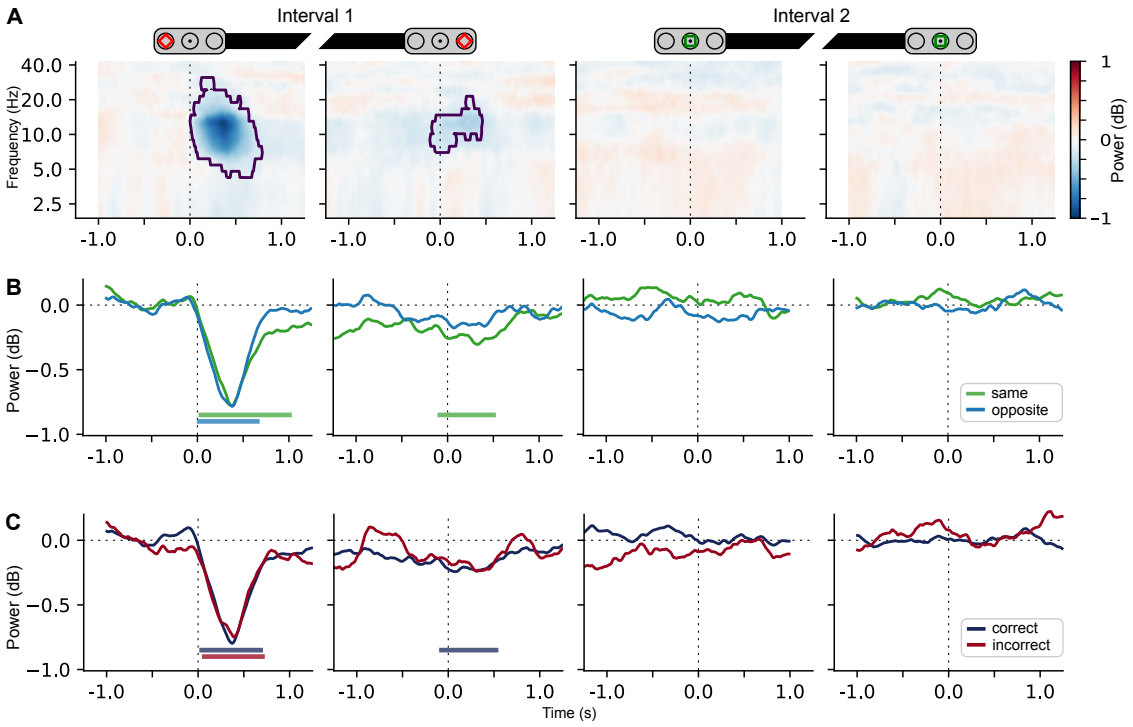

Figure 4. **A** Lateralized Time-frequency decomposition for the four consecutive epochs, from left to right. **B** Lateralized power in the alpha band, separately for 'Same' and 'Opposite' trials. **C** Lateralized power in the alpha band, separately for correct and incorrect trials.

Figure 4A depicts the full spectrum of lateralized power during each of the four epochs. In response to the onset of Interval 1, we found a large, significant cluster indicating contralateral power suppression. This cluster was centered around the alpha band, but extended to frequencies from approximately 5 to 20Hz. This is most likely due to the multitaper filtering, which typically has a high temporal accuracy, sometimes at the cost of more spectral bleeding. The onset of the cluster was almost immediately after stimulus onset, and it spanned approximately 750ms. Around the offset of Interval 1, similar contralateral suppression in the alpha band was found, albeit much lower in amplitude. Here, we found a cluster indicating significant suppression between 7 and 15Hz from -100 to +500ms. For Interval 2, during both the onset and offset epochs, no significant lateralization was found.

In Figure 4B, we have plotted the lateralized alpha power separately for 'Same' and 'Opposite' trials. In neither of the epochs any significant differences were found between

the two. Qualitatively, it seemed during Interval 1, 'Same' trials might have displayed slightly longer-lived alpha lateralization, persisting throughout the trial similar to the CDA component. For 'Opposite' trials, this was less apparent, with significant suppression only lasting up to approximately 600ms. Consequently, it seemed that at the end of the interval, suppression responses might be increased for 'Same' compared to 'Opposite' presentations, with no significant suppression for 'Opposite' trials. In the epochs surrounding Interval 2, no significant lateralization was found, in neither of these conditions. Figure 4C depicts the same time courses of lateralized alpha power separately for correct and incorrect responses. As with the ERPs, no significant differences were found in either of the epochs, and both trial types had very similar response profiles.

To conclude, the time-frequency analyses largely aligned with the ERP analyses: we found lateralized alpha suppression indicative of attentional orienting in response to the onset and offset markers of Interval 1. During Interval 2, there was no indication however that the location of these markers was attended or retrieved again.

Classification

The classification analyses explored whether marker locations were maintained or reactivated during comparison in a manner that was not captured by the previous analyses which focused on occipito-parietal electrodes. To this end, we trained a classifier to predict the location of onset or offset cues of Interval 1 from the broadband signal from all 64 channels. The outcome of this analysis is in line with the findings from the ERP- and time-frequency analyses. Figure 5 depicts, for each epoch, the performance of classifiers trained on the overall dataset, as well classifiers trained separately on 'Same' or 'Opposite' trials. The location of the onset- and offset markers could be decoded for a sustained period of time, with accuracies significantly above chance level from 109 to 984ms and from 109 to 1031 ms for onset and offset epochs, respectively. Separately classifying 'Same' and 'Opposite' trials yielded virtually identical results.

The decoding scores of these classifiers during the memory delay, depicted in the middle two panels of Figure 5 suggest that as the onset of Interval 2 draws closer the memory representation of the offset marker gradually dissipates. After the onset of the centrally presented Interval 2, none of the classifiers were able to accurately decode the marker locations of Interval 1. No more significant clusters of decoding performance were found.

To conclude, neither did the classification analyses provide any indication that the Interval 1 marker locations were memorized, retrieved, or otherwise represented during comparison.

Discussion

Many studies exploring the dynamics of working memory representations have made use of the finding that visual features of a stimulus appear to be bound to the location at which that stimulus was presented. That is, maintaining or retrieving non-spatial visual information has been found to evoke clear neural markers in the ERP and time-frequency spectra that are reflective of the location of presentation. Here, we investigated whether

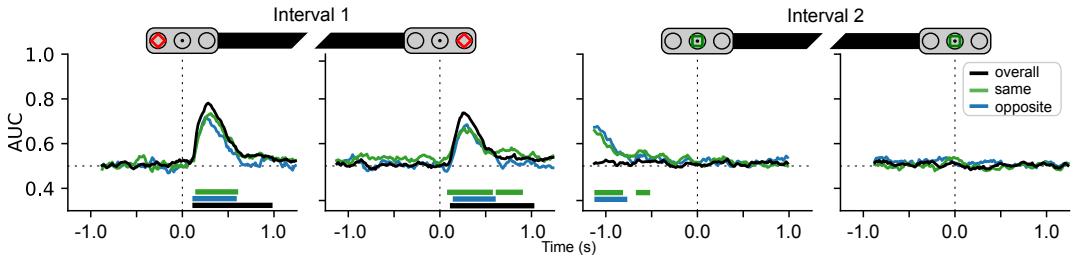

Figure 5. Classifier performance (Area Under the Curve) around the onset or offset of Interval 1 and Interval 2. For Interval 2-epochs, the target of classification was the location of the onset- or offset marker of Interval 1.

temporal information is similarly bound to spatial information during encoding, maintenance and retrieval, as this would allow for exploring the dynamics of temporal memory. Participants perceived an interval presented by means of lateralized start- and end-marker stimuli, and we found that the encoding of the interval indeed evoked spatial neural signatures typically associated with working memory retention. However, when this interval was subsequently compared to an interval with central markers, no signs of lateralization were found; neither in the ERP, nor in the time-frequency spectrum, nor could spatial information otherwise be decoded using multivariate pattern analysis. These results suggest that while memory for visual features such as location might play a role during initially timing an interval, spatial information is not involved when the interval is subsequently used for comparison.

The start marker of the first interval produced lateralized ERP components, lateralized alpha suppression, and sustained robust classification accuracies that are highly comparable to those found in typical studies on visual working memory encoding (Carlisle et al., 2011; de Vries et al., 2017; Gunseli et al., 2014; Van Driel et al., 2017; Wolff et al., 2017), which we interpret as signatures of working memory involvement in this timing task. One notable difference in the ERP is that from 300 to 400ms, we actually found a contralateral positivity where we had anticipated to find an N2pc-component. One could suspect that this discrepancy stems from the laterally unbalanced displays used in our design: in most working memory studies the lateralized memorandum is commonly presented alongside a nontarget in the opposite hemifield. Indeed, unilaterally presented highly salient stimuli have indeed sometimes been shown to evoke a so-called P2pc in this time window (Casiraghi, Fortier-Gauthier, Sessa, Dell'Acqua, & Jolicœur, 2013). However, based on comparisons to early investigations of the N2pc with displays that were similarly 'unbalanced' (Hickey, Di Lollo, & McDonald, 2009), we suggest that this positivity could also reflect a component known as a distractor positivity P_D (see also Burra & Kerzel, 2014; Sawaki & Luck, 2010, 2013). This might reflect how participants actively suppressed this salient onset in order to maintain central fixation. Critically, however, despite the initial 'distractor status' of the marker, the positivity still reversed into a sustained negativity that reflected a CDA.

The neural responses elicited by the end marker of the first interval were largely similar to those caused by its onset. Notably, the end marker resulted in a CDA-component that lasted well into the delay period, qualitatively even seeming to persist into the second

interval. If the CDA is caused by the working memory processes involved in timing, this raises the question why another CDA would arise after the 'timing work' is already done. One possible explanation would be that this signature reflects maintenance of the relevant duration during the delay interval. If this were the case, however, we would have anticipated a CDA-difference between 'Same' and 'Opposite' trials, where the former trial type would be much stronger associated with its location than the latter. Another explanation would be that the delay period in itself is actually an interval that is being timed, so as to optimally anticipate the start of the comparison interval.

Despite these lateralized neural signatures found during Interval 1, our results indicate that the central markers of Interval 2 did not convey any information regarding the preceding locations of Interval 1. One theoretical account that fits these results poses that while time perception may result from distributed intrinsic circuits, these circuits might subsequently project to more centralized 'readout neurons' who allow for the comparison of intervals across distributed clocks (Bakhurin et al., 2017; Laje & Buonomano, 2013; Paton & Buonomano, 2018). As such, the spatial code might be used in the initial perception of time, but not retained or retrieved when the interval is compared later on. Another, subtly different account would state that in order for the duration maintained in memory to be used in comparison, its representation needs to be actively transformed into a new representation. Such transformations have been proposed be necessary for visual search (Myers, Stokes, & Nobre, 2017), as it would allow for only the relevant items in memory to guide attentional selection without interference from others (see also Chatham, Frank, & Badre, 2014; Olivers, Peters, Houtkamp, & Roelfsema, 2011). However, one key difference is that for visual search there is strong evidence that transformed representations still make use of the spatial code (de Vries et al., 2018; de Vries et al., 2017, 2019), whereas for temporal information this association appears to be absent.

As such, our results do not unequivocally support either dedicated or intrinsic clock models. On the one hand, the dynamics observed during Interval 1 are in line with what one would predict following intrinsic models of time perception. However, the observation that the spatial code appears to be abandoned during comparison largely falls in line with dedicated models. Of note, our behavioral data yielded unexpected support for intrinsic clock models: the shift in perceived time between 'Same' and 'Opposite' blocks indicates that a relatively subtle difference in the manner of presentation can have a profound impact on the temporal percept (in line with Droit-Volet & Meck, 2007; Eagleman & Pariyadath, 2009; Johnston, Arnold, & Nishida, 2006; Matthews, 2011). This behavioral bias coincided with ERP differences in response to the offset markers of 'Same' and 'Opposite' markers, which is a finding that warrants more thorough exploration than the scope of this study allows. We discuss this observation in more detail in a companion article (Kruijne, Olivers & Van Rijn, manuscript in preparation).

The mechanisms by which we perceive sensory events, and the experience of the timing of these events are intertwined by necessity. The present results offer new, important insights into the interplay of stimulus representations and temporal representations during perception, maintenance, and subsequent comparisons of interval durations. Despite converging evidence that many features of visually presented stimuli are bound to spatial information when encoded in working memory, we found no evidence that maintaining and retrieving temporal information relied on such an associative link. These results offer criti-

cal constraints for models that not only aim to measure time, but also to subsequently use that measurement in upcoming goal-directed behaviors. In other words, these findings offer important considerations for theories of temporal cognition beyond the perception of time.

Acknowledgements

The authors would like to thank Philippa Johnson for her help in data acquisition, and would like to thank Joram van Driel for his help with analyses and the experimental design.

References

Addyman, C., French, R. M., & Thomas, E. (2016). Computational models of interval timing. *Current Opinion in Behavioral Sciences*. Time in perception and action, *8*, 140–146. doi:10.1016/j.cobeha.2016.01.004

Allman, M. J., Teki, S., Griffiths, T. D., & Meck, W. H. (2014). Properties of the internal clock: First- and second-order principles of subjective time. *Annual Review of Psychology*, *65*(1), 743–771. doi:10.1146/annurev-psych-010213-115117

Baayen, R. H., Davidson, D. J., & Bates, D. M. (2008). Mixed-effects modeling with crossed random effects for subjects and items. *Journal of Memory and Language*. Special Issue: Emerging Data Analysis, *59*(4), 390–412. doi:10.1016/j.jml.2007.12.005

Bakhurin, K. I., Goudar, V., Shobe, J. L., Claar, L. D., Buonomano, D. V., & Masmanidis, S. C. (2017). Differential encoding of time by prefrontal and striatal network dynamics. *Journal of Neuroscience*, *37*(4), 854–870. doi:10.1523/JNEUROSCI.1789-16.2016

Bigdely-Shamlo, N., Mullen, T., Kothe, C., Su, K.-M., & Robbins, K. A. (2015). The prep pipeline: Standardized preprocessing for large-scale eeg analysis. *Frontiers in Neuroinformatics*, *9*. doi:10.3389/fninf.2015.00016

Buhusi, C. V. & Meck, W. H. (2005). What makes us tick? functional and neural mechanisms of interval timing. *Nature Reviews Neuroscience*, *6*(10), 755–765. doi:10.1038/nrn1764

Burra, N. & Kerzel, D. (2014). The distractor positivity (pd) signals lowering of attentional priority: Evidence from event-related potentials and individual differences. *Psychophysiology*, *51*(7), 685–696. doi:10.1111/psyp.12215

Carlisle, N. B., Arita, J. T., Pardo, D., & Woodman, G. F. (2011). Attentional templates in visual working memory. *The Journal of Neuroscience*, *31*(25), 9315–9322. doi:10.1523/JNEUROSCI.1097-11.2011

Casiraghi, M., Fortier-Gauthier, U., Sessa, P., Dell'Acqua, R., & Jolicœur, P. (2013). N1pc reversal following repeated eccentric visual stimulation. *Psychophysiology*, *50*(4), 351–364. doi:10.1111/psyp.12021

Chatham, C. H., Frank, M. J., & Badre, D. (2014). Corticostriatal output gating during selection from working memory. *Neuron*, *81*(4), 930–942. doi:10.1016/j.neuron.2014.01.002

Coull, J. T., Cheng, R.-K., & Meck, W. H. (2011). Neuroanatomical and neurochemical substrates of timing. *Neuropsychopharmacology*, *36*(1), 3–25. doi:10.1038/npp.2010.113

Cousineau, D. (2005). Confidence intervals in within-subject designs: A simpler solution to loftus and masson's method. *Tutorials in Quantitative Methods for Psychology*, *1*(1), 42–45. doi:10.20982/tqmp.01.1.p042

de Vries, I. E. J., Van Driel, J., Karacaoglu, M., & Olivers, C. N. L. (2018). Priority switches in visual working memory are supported by frontal delta and posterior alpha interactions. *Cerebral Cortex*. doi:10.1093/cercor/bhy223

de Vries, I. E. J., Van Driel, J., & Olivers, C. N. L. (2017). Posterior α eeg dynamics dissociate current from future goals in working memory-guided visual search. *Journal of Neuroscience*, *37*(6), 1591–1603. doi:10.1523/JNEUROSCI.2945-16.2016

de Vries, I. E. J., Van Driel, J., & Olivers, C. N. L. (2019). Decoding the status of working memory representations in preparation of visual selection. *NeuroImage*, *191*, 549–559. doi:10.1016/j.neuroimage.2019.02.069

Dell'Acqua, R., Sessa, P., Toffanin, P., Luria, R., & Jolicœur, P. (2010). Orienting attention to objects in visual short-term memory. *Neuropsychologia*, *48*(2), 419–428. doi:10.1016/j.neuropsychologia.2009.09.033

Delorme, A. & Makeig, S. (2004). Eeglab: An open source toolbox for analysis of single-trial eeg dynamics including independent component analysis. *Journal of Neuroscience Methods*, *134*(1), 9–21. doi:10.1016/j.jneumeth.2003.10.009

Diepen, R. M. v., Miller, L. M., Mazaheri, A., & Geng, J. J. (2016). The role of alpha activity in spatial and feature-based attention. *eneuro*, *3*(5), ENEURO.0204–16.2016. doi:10.1523/ENEURO.0204-16.2016

Droit-Volet, S. & Meck, W. H. (2007). How emotions colour our perception of time. *Trends in Cognitive Sciences*, *11*(12), 504–513. doi:10.1016/j.tics.2007.09.008

Eagleman, D. M. (2008). Human time perception and its illusions. *Current Opinion in Neurobiology*. Cognitive neuroscience, *18*(2), 131–136. doi:10.1016/j.conb.2008.06.002

Eagleman, D. M. & Pariyadath, V. (2009). Is subjective duration a signature of coding efficiency? *Philosophical Transactions of the Royal Society B: Biological Sciences*, *364*(1525), 1841–1851. doi:10.1098/rstb.2009.0026

Eimer, M. (1993). Spatial cueing, sensory gating and selective response preparation: An erp study on visuo-spatial orienting. *Electroencephalography and Clinical Neurophysiology/Evoked Potentials Section*, *88*(5), 408–420.

Eimer, M. & Grubert, A. (2014). Spatial attention can be allocated rapidly and in parallel to new visual objects. *Current Biology*, *24*(2), 193–198. doi:10.1016/j.cub.2013.12.001

Eimer, M. & Kiss, M. (2010). An electrophysiological measure of access to representations in visual working memory. *Psychophysiology*, *47*(1), 197–200. doi:10.1111/j.1469-8986.2009.00879.x

Ernst, B., Reichard, S. M., Riepl, R. F., Steinhauser, R., Zimmermann, S. F., & Steinhauser, M. (2017). The p3 and the subjective experience of time. *Neuropsychologia*, *103*, 12–19. doi:10.1016/j.neuropsychologia.2017.06.033

Finnerty, G. T., Shadlen, M. N., Jazayeri, M., Nobre, A. C., & Buonomano, D. V. (2015). Time in cortical circuits. *Journal of Neuroscience*, *35*(41), 13912–13916. doi:10.1523/JNEUROSCI.2654-15.2015

Foster, J. J., Sutterer, D. W., Serences, J. T., Vogel, E. K., & Awh, E. (2017). Alpha-band oscillations enable spatially and temporally resolved tracking of covert spatial attention. *Psychological Science*, *28*(7), 929–941. doi:10.1177/0956797617699167

French, R. M., Addyman, C., Mareschal, D., & Thomas, E. (2014). Gamit - a fading-gaussian activation model of interval-timing: Unifying prospective and retrospective time estimation. *Timing & Time Perception Reviews*, *1*(1), 1–17. doi:10.1163/24054496-00101002

Gibbon, J. (1977). Scalar expectancy theory and weber's law in animal timing. *Psychological review*, *84*(3), 279.

Gramfort, A., Luessi, M., Larson, E., Engemann, D. A., Strohmeier, D., Brodbeck, C., ... Hämäläinen, M. (2013). Meg and eeg data analysis with mne-python. *Frontiers in Neuroscience*, *7*. doi:10.3389/fnins.2013.00267

Gramfort, A., Luessi, M., Larson, E., Engemann, D. A., Strohmeier, D., Brodbeck, C., ... Hämäläinen, M. S. (2014). Mne software for processing meg and eeg data. *NeuroImage*, *86*, 446–460. doi:10.1016/j.neuroimage.2013.10.027

Gu, B.-M., van Rijn, H., & Meck, W. H. (2015). Oscillatory multiplexing of neural population codes for interval timing and working memory. *Neuroscience & Biobehavioral Reviews*, *48*, 160–185. doi:10.1016/j.neubiorev.2014.10.008

Gunseli, E., Olivers, C. N. L., & Meeter, M. (2014). Effects of search difficulty on the selection, maintenance, and learning of attentional templates. *Journal of Cognitive Neuroscience*, *26*(9), 2042–2054. doi:10.1162/jocn_a_00600

Halbertsma, H. N. & Rijn, H. V. (2016). An evaluation of the effect of auditory emotional stimuli on interval timing. *Timing & Time Perception*, *4*(1), 48–62. doi:10.1163/22134468-00002061

Hass, J. & Durstewitz, D. (2014). Neurocomputational models of time perception. In H. Merchant & V. de Lafuente (Eds.), *Neurobiology of interval timing* (pp. 49–71). Advances in Experimental Medicine and Biology. New York, NY: Springer New York.

Hass, J. & Herrmann, J. M. (2012). The neural representation of time: An information-theoretic perspective. *Neural Computation*, *24*(6), 1519–1552. doi:10.1162/NECO_a_00280

Hickey, C., Di Lollo, V., & McDonald, J. J. (2009). Electrophysiological indices of target and distractor processing in visual search. *Journal of Cognitive Neuroscience*, *21*(4), 760–775. doi:10.1162/jocn.2009.21039

Ikkai, A., McCollough, A. W., & Vogel, E. K. (2010). Contralateral delay activity provides a neural measure of the number of representations in visual working memory. *Journal of Neurophysiology*, *103*(4), 1963–1968. doi:10.1152/jn.00978.2009

Jas, M., Engemann, D. A., Bekhti, Y., Raimondo, F., & Gramfort, A. (2017). Autoreject: Automated artifact rejection for meg and eeg data. *NeuroImage*, *159*, 417–429. doi:10.1016/j.neuroimage.2017.06.030

Jazayeri, M. & Shadlen, M. N. (2010). Temporal context calibrates interval timing. *Nature Neuroscience*, *13*(8), 1020–1026. doi:10.1038/nn.2590

Johnston, A., Arnold, D. H., & Nishida, S. (2006). Spatially localized distortions of event time. *Current Biology*, *16*(5), 472–479. doi:10.1016/j.cub.2006.01.032

Kacelnik, A., Brunner, D., & Gibbon, J. (1990). Timing mechanisms in optimal foraging: Some applications of scalar expectancy theory. In *Behavioural mechanisms of food selection* (pp. 61–82). Springer.

Klimesch, W. (2012). Alpha-band oscillations, attention, and controlled access to stored information. *Trends in Cognitive Sciences*, *16*(12), 606–617. doi:10.1016/j.tics.2012.10.007

Kuo, B.-C., Rao, A., Lepsien, J., & Nobre, A. C. (2009). Searching for targets within the spatial layout of visual short-term memory. *Journal of Neuroscience*, *29*(25), 8032–8038. doi:10.1523/JNEUROSCI.0952-09.2009

Laje, R. & Buonomano, D. V. [Dean V]. (2013). Robust timing and motor patterns by taming chaos in recurrent neural networks. *Nature Neuroscience*, *16*(7), 925–933. doi:10.1038/nn.3405

Lejeune, H. & Wearden, J. H. (2009). Vierordt's the experimental study of the time sense (1868) and its legacy. *European Journal of Cognitive Psychology*, *21*(6), 941–960. doi:10.1080/09541440802453006

Leszczyński, M., Myers, N. E., Akyürek, E. G., & Schubö, A. (2011). Recoding between two types of stm representation revealed by the dynamics of memory search. *Journal of Cognitive Neuroscience*, *24*(3), 653–663. doi:10.1162/jocn_a_00102

Lopez-Calderon, J. & Luck, S. J. (2014). Erplab: An open-source toolbox for the analysis of event-related potentials. *Frontiers in Human Neuroscience*, *8*. doi:10.3389/fnhum.2014.00213

Luck, S. J., Fan, S., & Hillyard, S. A. (1993). Attention-related modulation of sensory-evoked brain activity in a visual search task. *Journal of Cognitive Neuroscience*, *5*(2), 188–195.

Luck, S. J. & Hillyard, S. A. (1994). Electrophysiological correlates of feature analysis during visual search. *Psychophysiology*, *31*(3), 291–308. doi:10.1111/j.1469-8986.1994.tb02218.x

Luria, R., Balaban, H., Awh, E., & Vogel, E. K. (2016). The contralateral delay activity as a neural measure of visual working memory. *Neuroscience & Biobehavioral Reviews*, *62*, 100–108. doi:10.1016/j.neubiorev.2016.01.003

Lustig, C. & Meck, W. H. (2001). Paying attention to time as one gets older. *Psychological Science*, *12*(6), 478–484. doi:10.1111/1467-9280.00389

Maaß, S. C., Riemer, M., Wolbers, T., & van Rijn, H. (2019). Timing deficiencies in amnestic mild cognitive impairment: Disentangling clock and memory processes. *Behavioural Brain Research*, *373*, 112110. doi:10.1016/j.bbr.2019.112110

Maaß, S. C., Schlichting, N., & van Rijn, H. (2019). Eliciting contextual temporal calibration: The effect of bottom-up and top-down information in reproduction tasks. *Acta Psychologica*, *199*, 102898. doi:10.1016/j.actpsy.2019.102898

Malapani, C. & Fairhurst, S. (2002). Scalar timing in animals and humans. *Learning and Motivation*, *33*(1), 156–176. doi:10.1006/lmot.2001.1105

Maris, E. & Oostenveld, R. (2007). Nonparametric statistical testing of eeg- and meg-data. *Journal of Neuroscience Methods*, *164*(1), 177–190. doi:10.1016/j.jneumeth.2007.03.024

Matell, M. S. & Meck, W. H. (2004). Cortico-striatal circuits and interval timing: Coincidence detection of oscillatory processes. *Brain Research. Cognitive Brain Research*, *21*(2), 139–170. doi:10.1016/j.cogbrainres.2004.06.012

Mathôt, S., Schreij, D., & Theeuwes, J. (2012). Opensesame: An open-source, graphical experiment builder for the social sciences. *Behavior Research Methods*, *44*(2), 314–324. doi:10.3758/s13428-011-0168-7

Matthews, W. J. (2011). Stimulus repetition and the perception of time: The effects of prior exposure on temporal discrimination, judgment, and production. *PLOS ONE*, *6*(5), e19815. doi:10.1371/journal.pone.0019815

Mauk, M. D. & Buonomano, D. V. [Dean V.]. (2004). The neural basis of temporal processing. *Annual Review of Neuroscience*, *27*(1), 307–340. doi:10.1146/annurev.neuro.27.070203.144247

Mazaheri, A. (2010). Rhythmic pulsing: Linking ongoing brain activity with evoked responses. *Frontiers in Human Neuroscience*, *4*. doi:10.3389/fnhum.2010.00177

Meck, W. H. (1996). Neuropharmacology of timing and time perception. *Cognitive Brain Research*. Proceedings of the Fifth International Meeting of the European Behavioural Pharmacology Society (EBPS), *3*(3), 227–242. doi:10.1016/0926-6410(96)00009-2

Morey, R. D. (2008). Confidence intervals from normalized data: A correction to cousineau (2005). *Tutorials in Quantitative Methods for Psychology*, *4*(2), 61–64. doi:10.20982/tqmp.04.2.p061

Myers, N. E., Stokes, M. G., & Nobre, A. C. (2017). Prioritizing information during working memory: Beyond sustained internal attention. *Trends in Cognitive Sciences*, *21*(6), 449–461. doi:10.1016/j.tics.2017.03.010

Oberauer, K. & Lin, H.-Y. (2017). An interference model of visual working memory. *Psychological Review*, *124*(1), 21–59. doi:10.1037/rev0000044

Okamoto, H. & Fukai, T. (2001). Neural mechanism for a cognitive timer. *Physical Review Letters*, *86*(17), 3919–3922. doi:10.1103/PhysRevLett.86.3919

Olivers, C. N. L., Peters, J., Houtkamp, R., & Roelfsema, P. R. (2011). Different states in visual working memory: When it guides attention and when it does not. *Trends in Cognitive Sciences*, *15*(7), 327–334. doi:10.1016/j.tics.2011.05.004

Oostenveld, R., Fries, P., Maris, E., & Schoffelen, J.-M. (2011). Fieldtrip: Open source software for advanced analysis of meg, eeg, and invasive electrophysiological data. *Computational Intelligence and Neuroscience*, *2011*, 1–9. doi:10.1155/2011/156869

Paton, J. J. & Buonomano, D. V. [Dean V.]. (2018). The neural basis of timing: Distributed mechanisms for diverse functions. *Neuron*, *98*(4), 687–705. doi:10.1016/j.neuron.2018.03.045

Peirce, J. W. (2007). Psychopy-psychophysics software in python. *Journal of Neuroscience Methods*, *162*(1-2), 8–13. doi:10.1016/j.jneumeth.2006.11.017

Poch, C., Campo, P., & Barnes, G. R. (2014). Modulation of alpha and gamma oscillations related to retrospectively orienting attention within working memory. *European Journal of Neuroscience*, *40*(2), 2399–2405.

R Core Team. (2018). *R: A language and environment for statistical computing*. R Foundation for Statistical Computing. Vienna, Austria.

Ridgway, G. R., Litvak, V., Flandin, G., Friston, K. J., & Penny, W. D. (2012). The problem of low variance voxels in statistical parametric mapping; a new hat avoids a 'haircut'. *NeuroImage*, *59*(3), 2131–2141. doi:10.1016/j.neuroimage.2011.10.027

Roach, N. W., McGraw, P. V., Whitaker, D. J., & Heron, J. (2017). Generalization of prior information for rapid bayesian time estimation. *Proceedings of the National Academy of Sciences*, *114*(2), 412–417. doi:10.1073/pnas.1610706114

Sauseng, P., Klimesch, W., Stadler, W., Schabus, M., Doppelmayr, M., Hanslmayr, S., ... Birbaumer, N. (2005). A shift of visual spatial attention is selectively associated with human eeg alpha activity. *European Journal of Neuroscience*, *22*(11), 2917–2926. doi:10.1111/j.1460-9568.2005.04482.x

Sawaki, R. & Luck, S. J. (2010). Capture versus suppression of attention by salient singletons: Electrophysiological evidence for an automatic attend-to-me signal. *Attention, Perception, & Psychophysics*, *72*(6), 1455–1470. doi:10.3758/APP.72.6.1455

Sawaki, R. & Luck, S. J. (2013). Active suppression after involuntary capture of attention. *Psychonomic bulletin & review*, *20*(2), 296–301.

Schlichting, N., Damsma, A., Aksoy, E. E., Wächter, M., Asfour, T., & Rijn, H. v. (2018). Temporal context influences the perceived duration of everyday actions: Assessing the ecological validity of lab-based timing phenomena. *Journal of Cognition*, *1*(1), 4. doi:10.5334/joc.4

Schlichting, N., de Jong, R., & van Rijn, H. (2018). Performance-informed eeg analysis reveals mixed evidence for eeg signatures unique to the processing of time. *Psychological Research*. doi:10.1007/s00426-018-1039-y

Schneegans, S. & Bays, P. M. (2017). Neural architecture for feature binding in visual working memory. *Journal of Neuroscience*, *37*(14), 3913–3925. doi:10.1523/JNEUROSCI.3493-16.2017

Shankar, K. H. & Howard, M. W. (2010). Timing using temporal context. *Brain Research*. Computational Cognitive Neuroscience III: Selected presentations from CCNC-09, *1365*, 3–17. doi:10.1016/j.brainres.2010.07.045

Shankar, K. H. & Howard, M. W. (2011). A scale-invariant internal representation of time. *Neural Computation*, *24*(1), 134–193. doi:10.1162/NECO_a_00212

Shankar, K. H. & Howard, M. W. (2013). Optimally fuzzy temporal memory. *The Journal of Machine Learning Research*, *14*(1), 3785–3812.

Soares, S., Atallah, B. V., & Paton, J. J. (2016). Midbrain dopamine neurons control judgment of time. *Science*, *354*(6317), 1273–1277. doi:10.1126/science.aah5234

Swan, G. & Wyble, B. (2014). The binding pool: A model of shared neural resources for distinct items in visual working memory. *Attention, Perception, & Psychophysics*, *76*(7), 2136–2157. doi:10.3758/s13414-014-0633-3

Taatgen, N. & van Rijn, H. (2011). Traces of times past: Representations of temporal intervals in memory. *Memory & Cognition*, *39*(8), 1546–1560. doi:10.3758/s13421-011-0113-0

Tan, M. & Wyble, B. (2015). Understanding how visual attention locks on to a location: Toward a computational model of the n2pc component. *Psychophysiology*, *52*(2), 199–213. doi:10.1111/psyp.12324

Turgeon, M., Lustig, C., & Meck, W. H. (2016). Cognitive aging and time perception: Roles of bayesian optimization and degeneracy. *Frontiers in Aging Neuroscience*, *8*. doi:10.3389/fnagi.2016.00102

Van Driel, J., Gunseli, E., Meeter, M., & Olivers, C. N. L. (2017). Local and interregional alpha eeg dynamics dissociate between memory for search and memory for recognition. *NeuroImage*, *149*, 114–128. doi:10.1016/j.neuroimage.2017.01.031

van Ede, F. (2018). Mnemonic and attentional roles for states of attenuated alpha oscillations in perceptual working memory: A review. *The European journal of neuroscience*, *48*(7), 2509–2515. doi:10.1111/ejn.13759

van Ede, F., Niklaus, M., & Nobre, A. C. (2017). Temporal expectations guide dynamic prioritization in visual working memory through attenuated α oscillations. *Journal of Neuroscience*, *37*(2), 437–445. doi:10.1523/JNEUROSCI.2272-16.2017

van Moorselaar, D., Foster, J. J., Sutterer, D. W., Theeuwes, J., Olivers, C. N. L., & Awh, E. (2018). Spatially selective alpha oscillations reveal moment-by-moment trade-offs between working memory and attention. *Journal of cognitive neuroscience*, *30*(2), 256–266. doi:10.1162/jocn_a_01198

van Rijn, H., Gu, B.-M., & Meck, W. H. (2014). Dedicated clock/timing-circuit theories of time perception and timed performance. In H. Merchant & V. de Lafuente (Eds.), *Neurobiology of interval timing* (pp. 75–99). Advances in Experimental Medicine and Biology. New York, NY: Springer New York.

Vogel, E. K. & Machizawa, M. G. (2004). Neural activity predicts individual differences in visual working memory capacity. *Nature*, *428*(6984), 748–751. doi:10.1038/nature02447

Walsh, V. (2003). A theory of magnitude: Common cortical metrics of time, space and quantity. *Trends in Cognitive Sciences*, *7*(11), 483–488. doi:10.1016/j.tics.2003.09.002

Wolff, M. J., Jochim, J., Akyürek, E. G., & Stokes, M. G. (2017). Dynamic hidden states underlying working-memory-guided behavior. *Nature Neuroscience*, *advance online publication*. doi:10.1038/nn.4546

Woodman, G. F., Carlisle, N. B., & Reinhart, R. M. (2013). Where do we store the memory representations that guide attention? *Journal of vision*, *13*(3), 1.